## Comparison of Model Order Reduction Techniques for Flexible Multibody Dynamics using an Equivalent Rigid-Link System Approach

(Article begins on next page)

21 February 2025

# Comparison of Model Order Reduction Techniques for Flexible Multibody Dynamics using an Equivalent Rigid-Link System Approach

Renato Vidoni[1], Lorenzo Scalera[2], Alessandro Gasparetto[2], Marco Giovagnoni[2]

[1] Faculty of Science and Technology
Free University of Bozen-Bolzano
piazza Università 5, 39100, Bolzano, Italy
renato.vidoni@unibz.it

[2] DPIA, Polytechnic Department
of Engineering and Architecture
University of Udine
Via delle Scienze, 208, 33100, Udine, Italy
scalera.lorenzo@spes.uniud.it
alessandro.gasparetto@uniud.it
giovagnoni@uniud.it

## Abstract

In this paper we present a comparison of different model order reduction techniques for flexible multibody dynamics. In particular, we adopt a formulation based on a Equivalent Rigid-Link System (ERLS). This approach is suitable in the case of large displacements and small elastic deformations and it allows the kinematic equations of motion to be decoupled from the compatibility equations of the displacements at the joints. The ERLS approach, recently extended through a modal formulation, is here implemented in combination with different reduction techniques, i.e. Craig-Bampton, Interior Mode Ranking (IMR), Guyan, Least Square Model Reduction (LSMR) and Mode Displacement Method (MDM). In order to assess the advantages and disadvantages of the different methodologies, these techniques are applied to a benchmark mechanism under different input conditions, i.e. gravitational force and step torque input. The accuracy of each reduced model is numerically evaluated through the comparison of computational time, the behaviour in frequency domain and by means of vector correlation methods, i.e. Modal Assurance Criterion (MAC), Cross-Orthogonality (CO) and Normalized Cross-Orthogonality (NCO).

**Keywords:** Equivalent Rigid-Link System, Flexible Multibody Dynamics, Model Order Reduction, flexible-link mechanism

## 1. Introduction

Nowadays, industrial mechanisms and robots are demanded to be lightweight, easily manoeuvrable and less energy-intensive. These features result in the design of manipulators in which structural flexibility has to be taken into account and, therefore, simulation and control become more difficult and challenging. For these reasons, not only the kinematics [7], but also the dynamic modelling of flexible multibody systems [21] has become, in the last decades, a crucial research topic in both industry and academia and it is still an open field of investigation.

In multibody dynamics, the classical approach to take into account the flexibility of elastic mechanisms is based on the rigid-body dynamical model of the system and then the elastic deformations are introduced. The elastic deformations of the bodies are influenced by the rigid motion and vice versa. It results in a highly non-linear dynamic formulation described by a coupled set of partial differential equations. Two main methodologies can be found in literature for obtaining a set of ordinary differential equations: the nodal approach (i.e. the Finite Element Method, FEM) and the modal one [20]. However, since a high number of Degrees of Freedom (DoFs) is introduced by the discretization of the flexible bodies, proper reduction methods should be applied in order to allow an efficient simulation of the multibody system while keeping an accurate description of the predominant dynamic behaviour.

Model reduction methods can be classified in physical coordinates techniques, generalized coordinates (i.e. modal coordinates) and hybrid methods, such as the Component Mode Synthesis (CMS). A review of model reduction techniques for structural dynamics, numerical mathematics and system and control is proposed in [4], whereas in [2], [9] and [18] reduced order modelling strategies are applied in dynamics sub-structuring. An example of model reduction can be found in [12], in which a study on an elastic rod is proposed. Furthermore, in the field of multibody systems, an overview of the basic approaches to model elastic multibody systems with the help of Floating Frame of Reference formulation in given by [14]. A new ranking method (Interior Mode Ranking, IMR) for the selection of interior normal modes in the Craig-Bampton technique [3] has been proposed in [15].

In this work, an Equivalent Rigid-Link System (ERLS) formulation for modelling the dynamics of flexible multibody systems is considered in its recent developments. This approach, suitable in case of large displacements and small elastic deformations, differently from other formulations, e.g. the Floating Frame of Reference (FFR) [20], enables the

kinematic equations of the ERLS to be decoupled from the compatibility equations of the displacement at the joints. In previous works, the ERLS approach has been firstly applied to model planar flexible-link mechanisms and then 3D flexible systems [22] [23]. The ERLS formulation has been also exploited for simulation and control purposes [8] [10]. The evolution of the ERLS-based dynamic model for flexible mechanisms and its applications over the years have been presented in [5]. It has to be noticed that, if a computational time adequate for real-time simulation or control purposes is needed, the number of DoFs in the ERLS-FEM model (i.e. the number of nodes) should be kept low. For this reason, the ERLS formulation has been recently extended through a modal approach so as to obtain a more flexible solution based on a reduced-order system of equations and, in particular, a classical Craig-Bampton approach has been adopted [21]. However, this reduction is not the only technique capable of reducing the number of DoFs.

For this reason, in this paper different model order reduction techniques are implemented using the ERLS approach and the results compared. In particular, we evaluate advantages and disadvantages of the different techniques on a L-shaped benchmark mechanism under different input conditions. FEM models of the benchmark mechanism are developed in Ansys® environment with different discretizations, whereas dynamics and post-processing are evaluated by means of Matlab™ software. The reduced model accuracy is evaluated through the comparison of the computational time, the accuracy in frequency domain and by means of vector correlation methods such as Modal Assurance Criterion [1] [16] [18], Cross-Orthogonality [1] and Normalized Cross-Orthogonality [13] [15] [24].

The paper is organized as follows: in Section 2 the Equivalent Rigid-Link System kinematics and dynamics formulation is presented; in Section 3 the model order reduction techniques, that have been implemented and tested on the ERLS dynamic model, are briefly recalled; Section 4 shows the numerical implementation of the model on a benchmark mechanism, whereas in Section 5 the results of the simulations are presented and discussed. Finally, Section 6 gives the conclusions of this work.

## 2. Equivalent Rigid-Link System modal formulation

### 2.1. ERLS kinematics

In this section, the Equivalent Rigid-Link System modal formulation, presented and evaluated in [21], is briefly recalled and summarized. With reference to Fig.1, the kinematic definitions of the Equivalent Rigid-Link System can be introduced: $\boldsymbol{u}_{i,k}$ represents the $k$-th nodal displacement vector of the $i$-th link, $\boldsymbol{e}_{i,k}$ the $k$-th nodal position vector for the $i$-th link of the ERLS, whereas $\boldsymbol{p}_{i,k}$ the absolute nodal position vector, that can be computed as:

$$\boldsymbol{p}_{i,k} = \boldsymbol{e}_{i,k} + \boldsymbol{u}_{i,k} \tag{1}$$

The index $i$ spans from 1 to $N$, i.e. the number of links of the mechanism, whereas $k$ spans from 1 to $h$, i.e. the number of nodes of the $i$-th link. In Fig.1, $x$, $y$, $z$ is a fixed global reference frame, whereas $x_i$, $y_i$, $z_i$ is a local reference frame, fixed to the ERLS.
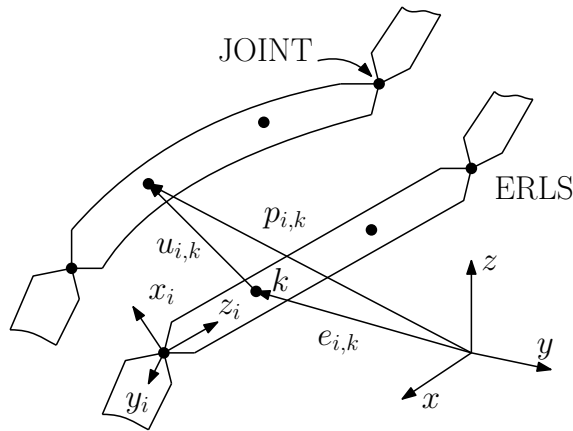


Figure 1: Kinematic definitions of the Equivalent Rigid-Link System.

The ERLS modal formulation can be developed starting from the expression of the nodal displacements $\boldsymbol{u}_i$ of the $i$-th link as functions of a given number of eigenvectors $\boldsymbol{U}_i$ and modal coordinates $\boldsymbol{q}_i$, as follows:

$$\boldsymbol{u}_i = \boldsymbol{U}_i \boldsymbol{q}_i \tag{2}$$

The eigenvectors and eigenvalues can be obtained accordingly to the chosen modal reduction technique, e.g. in our case Craig-Bampton, Interior Mode Ranking, Guyan, Least Square Model Reduction and Mode Displacement Method.

Let us consider two consequent links $i$ and $i+1$. The joint displacements belonging to each link are given by $\hat{u}_i = S_i U_i q_i$ and $\hat{u}_{i+1} = S_{i+1} U_{i+1} q_{i+1}$ respectively, where $S_i$ and $S_{i+1}$ are selection matrices introduced to extract the proper joint displacements from all the nodal displacements $u_i$. The compatibility condition at the $i$-th joint of the mechanism is given by:

$$\hat{u}_{i+1} = T_{i+1}\hat{u}_i \tag{3}$$

where $T_{i+1}(\boldsymbol{\theta})$ is a local-to-local transformation matrix between the two consecutive local reference frames associated to links $i$ and $i+1$. Note that Eq.(3) is linear with respect to modal coordinates. By writing the compatibility equations for all the links and assembling them in matrix format, the comprehensive compatibility equation can be obtained:

$$C(\boldsymbol{\theta})q = 0 \tag{4}$$

The coefficient matrix $C$ depends only on the joint parameters and the vector $q$ contains both the rigid and elastic modal coordinates. The rigid-body modal coordinates and elastic ones can be gathered into two separated vectors $q_r$ and $q_d$, respectively. In this manner, the compatibility equation can be rewritten in the following form:

$$C_r q_r + C_d q_d = 0 \tag{5}$$

The previous system can be solved with respect to $q_r$, by using the right pseudo-inverse matrix $C_r^+$, namely:

$$q_r = D(\boldsymbol{\theta})q_d \tag{6}$$

where matrix $D$ is defined as:

$$D = -C_r^+(\boldsymbol{\theta})C_d(\boldsymbol{\theta}) \tag{7}$$

$C_r^+$ and $C_d$ contain the coefficients of the rigid and vibrational modal coordinates respectively and only depend on the joint parameters vector $\boldsymbol{\theta}$. Starting from Eq.(6), the relationships between the velocities/virtual displacements and the accelerations of the independent variables can be derived. In particular, the following equations are obtained:

$$\dot{q}_r = D(\boldsymbol{\theta})\dot{q}_d + G(\boldsymbol{\theta}, q)\dot{\boldsymbol{\theta}} \tag{8}$$

$$\ddot{q}_r = G(\boldsymbol{\theta}, q)\ddot{\boldsymbol{\theta}} + D(\boldsymbol{\theta})\ddot{q}_d + n(\boldsymbol{\theta}, \dot{\boldsymbol{\theta}}, q, \dot{q}) \tag{9}$$

where the matrices $G$ and $n$ take into account the different contributions and dependencies.

## 2.2. ERLS dynamics

The dynamic equations are obtained by applying the principle of virtual work and computing the inertial, elastic, gravity and external generalized forces terms as follows:

$$\delta W_{inertia} + \delta W_{elastic} + \delta W_{gravity} + \delta W_{ext.forces} = 0 \tag{10}$$

Starting from Eq.(8), the virtual term of the generic $i$-th link, composed by the linear $\delta P_{0i}$, angular $\delta\boldsymbol{\phi}_i$ and modal $\delta q$ contributes, can be obtained as follows (see [21] for further details):

$$\begin{bmatrix} \delta P_{0i} \\ \delta\boldsymbol{\phi}_i \\ \delta q \end{bmatrix} = \begin{bmatrix} V_{\theta i} & 0 & 0 \\ 0 & V_{qri} & 0 \\ 0 & 0 & V_{qdi} \end{bmatrix} \begin{bmatrix} J(\boldsymbol{\theta}) & 0 \\ G(\boldsymbol{\theta},q) & D(\boldsymbol{\theta}) \\ 0 & I \end{bmatrix} \begin{bmatrix} \delta\boldsymbol{\theta} \\ \delta q_d \end{bmatrix} = V_i^o N \begin{bmatrix} \delta\boldsymbol{\theta} \\ \delta q_d \end{bmatrix} \tag{11}$$

where $V_i^o$ is a selection matrix for the proper elements of the $i$-th link ($V_{\theta i}$ is the selection block-matrix for the rigid DoF, $V_{qri}$ for the rigid modal coordinates and $V_{qdi}$ for the elastic modal ones) and $J(\boldsymbol{\theta})$ the Jacobian matrix of the Equivalent Rigid-Link System. The $V_i^o$ matrix is block diagonal and allows to select the correct terms related to both the rigid DoFs and the independent vibration modal coordinates.

The acceleration terms, i.e. linear $a_{0i}$, angular $\boldsymbol{\alpha}_i$ and modal $\ddot{q}$, can be rewritten, starting from Eq.(9), as function of the independent variables:

$$\begin{bmatrix} a_{0i} \\ \boldsymbol{\alpha}_i \\ \ddot{q} \end{bmatrix} = V_i^o N \begin{bmatrix} \ddot{\boldsymbol{\theta}} \\ \ddot{q}_d \end{bmatrix} + V_i^o \begin{bmatrix} \dot{J}(\boldsymbol{\theta}, \dot{\boldsymbol{\theta}})\dot{\boldsymbol{\theta}} \\ n(\boldsymbol{\theta}, \dot{\boldsymbol{\theta}}, q, \dot{q}) \\ 0 \end{bmatrix} \tag{12}$$

where $\dot{J}(\boldsymbol{\theta}, \dot{\boldsymbol{\theta}})$ represents the first time derivative of the Jacobian matrix of the ERLS. The second term of the equation depends only on the position and velocity of the independent variables and thus it is known.

The virtual work done by the inertial forces can be split into two contributes:

$$\delta \boldsymbol{W}_{inertia} = \delta \boldsymbol{W}_{inertia}^{I} + \delta \boldsymbol{W}_{inertia}^{II} \tag{13}$$

where the former contains all the terms related to the second derivative of the variables, the latter contains all the remaining terms. The virtual work done by the inertial forces $\delta \boldsymbol{W}_{inertia,i}^{I}$ and $\delta \boldsymbol{W}_{inertia,i}^{II}$ of each $i$-th link, and the virtual works done by the gravitational $\delta \boldsymbol{W}_{g}$ and generalized forces $\delta \boldsymbol{W}_{ext.forces}$, can be written as:

$$-\delta \boldsymbol{W}_{inertia,i}^{I} = \begin{bmatrix} \delta \boldsymbol{P}_{0i}^{T} & \delta \boldsymbol{\phi}_{i}^{T} & \delta \boldsymbol{q}^{T} \end{bmatrix} \mathbf{L}_{i} \begin{bmatrix} \boldsymbol{a}_{0i} \\ \boldsymbol{\alpha}_{i} \\ \ddot{\boldsymbol{q}} \end{bmatrix} \tag{14}$$

where the $\boldsymbol{L}_{i}$ matrix contains all the terms not depending on virtual displacements and accelerations.
By substituting Eq.(11) and (12) into Eq.(14), we can obtain:

$$-\delta \boldsymbol{W}_{inertia,i}^{I} = \begin{bmatrix} \delta \boldsymbol{\theta}^{T} & \delta \boldsymbol{q}_{d}^{T} \end{bmatrix} \boldsymbol{N}^{T} \boldsymbol{V}_{i}^{oT} \boldsymbol{L}_{i} \left( \boldsymbol{V}_{i}^{o} \boldsymbol{N} \begin{bmatrix} \ddot{\boldsymbol{\theta}} \\ \ddot{\boldsymbol{q}}_{d} \end{bmatrix} + \boldsymbol{V}_{i}^{o} \begin{bmatrix} \dot{\boldsymbol{J}}(\boldsymbol{\theta}, \dot{\boldsymbol{\theta}}) \dot{\boldsymbol{\theta}} \\ \boldsymbol{n}(\boldsymbol{\theta}, \dot{\boldsymbol{\theta}}, \boldsymbol{q}, \dot{\boldsymbol{q}}) \\ \boldsymbol{0} \end{bmatrix} \right) \tag{15}$$

The $\delta \boldsymbol{W}_{inertia,i}^{II}$ term can be expressed by gathering in the matrix $\boldsymbol{l}_{i}$ all the terms not depending on virtual displacements:

$$\delta \boldsymbol{W}_{inertia,i}^{II} = \begin{bmatrix} \delta \boldsymbol{P}_{0i}^{T} & \delta \boldsymbol{\phi}_{i}^{T} & \delta \boldsymbol{q}^{T} \end{bmatrix} \boldsymbol{l}_{i} = \begin{bmatrix} \delta \boldsymbol{\theta}^{T} & \delta \boldsymbol{q}_{d}^{T} \end{bmatrix} \boldsymbol{N}^{T} \boldsymbol{V}_{i}^{oT} \boldsymbol{l}_{i} \tag{16}$$

All the other terms such as the variation of the elastic energy $\delta \boldsymbol{H}$, the gravitational forces $\delta \boldsymbol{W}_{g}$ and the resultant generalized forces $\delta \boldsymbol{W}_{ext.forces}$ do not depend on accelerations. Then, they can be gathered into a unique term $\tilde{\boldsymbol{l}}_{i}$. By naming $\delta \boldsymbol{W}_{i}$ the term with all the contributions not depending on accelerations, it holds:

$$\delta \boldsymbol{W}_{i} = \begin{bmatrix} \delta \boldsymbol{P}_{0i}^{T} & \delta \boldsymbol{\phi}_{i}^{T} & \delta \boldsymbol{q}^{T} \end{bmatrix} \tilde{\boldsymbol{l}}_{i} = \begin{bmatrix} \delta \boldsymbol{\theta}^{T} & \delta \boldsymbol{q}_{d}^{T} \end{bmatrix} \boldsymbol{N}^{T} \boldsymbol{V}_{i}^{oT} \tilde{\boldsymbol{l}}_{i} \tag{17}$$

By adding up the contributions of all the $N$ links, the following formulation is obtained:

$$-\delta \boldsymbol{W}_{inertia}^{I} = \sum_{i=1}^{N} \begin{bmatrix} \delta \boldsymbol{\theta}^{T} & \delta \boldsymbol{q}_{d}^{T} \end{bmatrix} \boldsymbol{N}^{T} \boldsymbol{V}_{i}^{oT} \boldsymbol{L}_{i} \left( \boldsymbol{V}_{i}^{o} \boldsymbol{N} \begin{bmatrix} \ddot{\boldsymbol{\theta}} \\ \ddot{\boldsymbol{q}}_{d} \end{bmatrix} + \boldsymbol{V}_{i}^{o} \begin{bmatrix} \dot{\boldsymbol{J}}(\boldsymbol{\theta}, \dot{\boldsymbol{\theta}}) \dot{\boldsymbol{\theta}} \\ \boldsymbol{n}(\boldsymbol{\theta}, \dot{\boldsymbol{\theta}}, \boldsymbol{q}, \dot{\boldsymbol{q}}) \\ \boldsymbol{0} \end{bmatrix} \right) == \delta \boldsymbol{W} = \sum_{i=1}^{N} \begin{bmatrix} \delta \boldsymbol{\theta}^{T} & \delta \boldsymbol{q}_{d}^{T} \end{bmatrix} \boldsymbol{N}^{T} \boldsymbol{V}_{i}^{oT} \tilde{\boldsymbol{l}}_{i} \tag{18}$$

Finally, by naming $\boldsymbol{L} \stackrel{\text{def}}{=} \sum_{i=1}^{N} \boldsymbol{V}_{i}^{oT} \boldsymbol{L}_{i} \boldsymbol{V}_{i}^{o}$ and $\tilde{\boldsymbol{l}} \stackrel{\text{def}}{=} \sum_{i=1}^{N} \boldsymbol{V}_{i}^{oT} \tilde{\boldsymbol{l}}_{i}$, and discarding the virtual displacements, the final dynamic model results:

$$\boldsymbol{N}^{T} \boldsymbol{L} \boldsymbol{N} \begin{bmatrix} \ddot{\boldsymbol{\theta}} \\ \ddot{\boldsymbol{q}}_{d} \end{bmatrix} = \boldsymbol{N}^{T} \left( \boldsymbol{L} \left( - \begin{bmatrix} \dot{\boldsymbol{J}}(\boldsymbol{\theta}, \dot{\boldsymbol{\theta}}) \boldsymbol{\theta} \\ \boldsymbol{n}(\boldsymbol{\theta}, \dot{\boldsymbol{\theta}}, \boldsymbol{q}, \dot{\boldsymbol{q}}) \\ \boldsymbol{0} \end{bmatrix} \right) + \tilde{\boldsymbol{l}} \right) \tag{19}$$

## 3. Model Order Reduction Techniques

In this section, the techniques that have been implemented for the Model Order Reduction (MOR) of the ERLS-based dynamic model are briefly recalled. Starting from a generic dynamic equilibrium equation:

$$\boldsymbol{M} \ddot{\boldsymbol{X}}(t) + \boldsymbol{C} \dot{\boldsymbol{X}}(t) + \boldsymbol{K} \boldsymbol{X}(t) = \boldsymbol{F}(t) \tag{20}$$

where $\boldsymbol{M}$, $\boldsymbol{C}$, $\boldsymbol{K}$ are the mass, dumping and stiffness matrices, $\boldsymbol{X}$ is the independent coordinates vector and $\boldsymbol{F}$ is the force vector acting on the system, several MOR techniques assume the form of a coordinate transformation such as:

$$\boldsymbol{X}(t) = \boldsymbol{T} \boldsymbol{Z}(t) \tag{21}$$

where $\boldsymbol{T}$ is the transformation matrix that converts the reduced model coordinates $\boldsymbol{Z}$ in the complete model ones $\boldsymbol{X}$.

### 3.1. Craig-Bampton

Craig-Bampton is the classical modal reduction technique in multibody dynamics [3] [18]. It is a hybrid method that belongs to the Component Mode Synthesis techniques. By considering the partition of the degrees of freedom in two

sets: the boundary *B* DoFs, where the reduced link will be interfaced with other components of the structure, and the interior *I* DoFs, the link dynamic equation, without considering the damping, becomes:

$$\begin{bmatrix} M_{BB} & M_{BI} \\ M_{IB} & M_{II} \end{bmatrix} \begin{Bmatrix} \ddot{X}_B \\ \ddot{X}_I \end{Bmatrix} + \begin{bmatrix} K_{BB} & K_{BI} \\ K_{IB} & K_{II} \end{bmatrix} \begin{Bmatrix} X_B \\ X_I \end{Bmatrix} = \begin{Bmatrix} F_B \\ F_I \end{Bmatrix} \tag{22}$$

The transformation matrix $T_{CB}$, between physical and Craig-Bampton coordinates, can be obtained as follows:

$$X = \begin{Bmatrix} X_B \\ X_I \end{Bmatrix} = \begin{bmatrix} I & 0 \\ \varphi_C & \varphi_N \end{bmatrix} \begin{Bmatrix} q_C \\ q_N \end{Bmatrix} = T_{CB} \begin{Bmatrix} q_C \\ q_N \end{Bmatrix} \tag{23}$$

In the transformation matrix the first column partition is related to the constraint modes. These describe the motion of the system when each boundary degree of freedom undergoes a unit displacement, while holding the other boundary DoFs fixed. The second column partition is related to the fixed-boundary modes, that can be described as the interior DoF motion when the interface is fixed. The number of fixed-interface modes can be reduced in order to decrease the total number of DoFs. Finally, $q_C$ and $q_N$ are the reduced model coordinates corresponding to the constraint and to the fixed-boundary normal modes respectively.

### 3.2. Interior Mode Ranking

The Interior Mode Ranking (IMR) [15] is a technique developed for the selection of the interior normal modes in the Craig-Bampton reduction technique. The IMR method allows ranking the interior modes analytically by comparing their single contributions to the dynamics of interest of the complete system, given the actual boundary conditions. In the IMR approach (see [15] for the full development) a weighted participation coefficient $\gamma$ is defined for each considered interior mode $\zeta$:

$$\gamma_{\Lambda,\zeta} = \sum_{i \in \Lambda} \frac{|\gamma_{i,\zeta}|}{||\gamma_i||} \alpha_i \qquad \zeta = 1, ..., s \qquad \sum_{i \in \Lambda} \alpha_i = 1 \tag{24}$$

where $\Lambda$ is the set of the full system vibrational modes to be represented and $\gamma_i$ is the vector whose entries are the coefficients $\gamma_{i,\zeta}$. Furthermore, $\alpha_i$ is a normalized weighting coefficient referring to the *i*-th mode, employed to define the level of importance of each mode with respect to the reduced model. The larger the value of the coefficients $\gamma_{\Lambda,\zeta}$, the more the dynamics of the $\zeta$-th interior mode affects the full system. The modes retained are those with the largest values of the weighted participation coefficients. In the IMR reduction here adopted, we define the number of interior modes to be retained and we assign an equal weighting coefficient to all of them.

### 3.3. Guyan's reduction

Guyan is a physical-type reduction technique and it is based on the assumption that the effect of inertial forces on the eliminated physical coordinates is negligible [11] [19]. After grouping the DOFs corresponding to master (denoted by subscript *m*) and slave (subscript *s*), the equation of motion can be expressed as follows:

$$\begin{bmatrix} M_{mm} & M_{ms} \\ M_{sm} & M_{ss} \end{bmatrix} \begin{Bmatrix} \ddot{X}_m \\ \ddot{X}_s \end{Bmatrix} + \begin{bmatrix} K_{mm} & K_{ms} \\ K_{sm} & K_{ss} \end{bmatrix} \begin{Bmatrix} X_m \\ X_s \end{Bmatrix} = \begin{Bmatrix} F_m \\ 0 \end{Bmatrix} \tag{25}$$

Neglecting the inertia associated with the slave DoFs, it holds:

$$X_s = -K_{ss}^{-1} K_{sm} X_m \tag{26}$$

Finally, eliminating $X_s$ from Eq.(25), the transformation matrix can be obtained as:

$$T_G = \begin{bmatrix} I \\ -K_{ss}^{-1} K_{sm} \end{bmatrix} \tag{27}$$

### 3.4. Least Square Model Reduction

The Least Square Model Reduction (LSMR) [17] is a physical coordinates reduction technique, mode type. It is based on the subdivision of the eigenvectors into master *m* and slave *s* components, depending on their reference to master or slave DoFs. Starting from Eq.(20), the displacement vector $X$ may be expressed as:

$$X(t) = \Phi q(t) \tag{28}$$

where $\boldsymbol{\Phi}$ is the complete eigenvector matrix of the full model and $\boldsymbol{q}$ is the modal coordinates vector. If a modal truncation is applied in order to reduce the computation of the complete eigenvector matrix and only $p$ eigenvectors of the full model are retained, Eq.(28) is rewritten as:

$$\boldsymbol{X}(t) = \boldsymbol{\Phi}_p \boldsymbol{q}_p(t) \tag{29}$$

and it can be partitioned as:

$$\boldsymbol{X}(t) = \begin{Bmatrix} \boldsymbol{X}_m(t) \\ \boldsymbol{X}_s(t) \end{Bmatrix} = \begin{Bmatrix} \boldsymbol{\Phi}_{mp} \\ \boldsymbol{\Phi}_{sp} \end{Bmatrix} \boldsymbol{q}_p(t) \tag{30}$$

The transformation matrix for the LSMR technique is finally given by:

$$\boldsymbol{T}_{LSMR} = \begin{bmatrix} \boldsymbol{I} \\ \boldsymbol{\Phi}_{sp} \boldsymbol{\Phi}_{mp}^+ \end{bmatrix} \tag{31}$$

### 3.5. Mode Displacement Method

The Mode Displacement Method (MDM) [4] is a modal coordinates reduction technique, that consists in a truncation of high frequency modes. In the case of maintaining $m$ modes among the $n$ of the full model, it holds:

$$\boldsymbol{X} = \sum_{j=1}^{m} \boldsymbol{\Phi}_j \boldsymbol{q}_j + \sum_{j_r=m+1}^{n} \boldsymbol{\Phi}_{j_r} \boldsymbol{q}_{j_r} \tag{32}$$

where the second contribution of the right side of the equation corresponds to the deleted vibration modes.

### 4. Numerical simulations on a benchmark mechanism

The Equivalent Rigid-Link System formulation, in combination with the MOR techniques presented in Sect. 3, have been implemented in Matlab$^{TM}$ environment on a L-shaped benchmark mechanism [6] [21], shown in Fig. 2. The two rods that compose the L-mechanism are made of aluminium (density $\rho = 2700\ Kg/m^3$, Poisson's ratio $\nu = 0.33$, Young's module $E = 7e10^{10}\ N/m^2$), they are 500 $mm$ long, 8 $mm$ wide and 8 $mm$ deep.
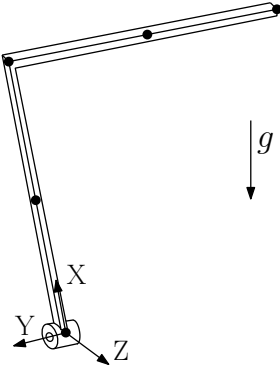


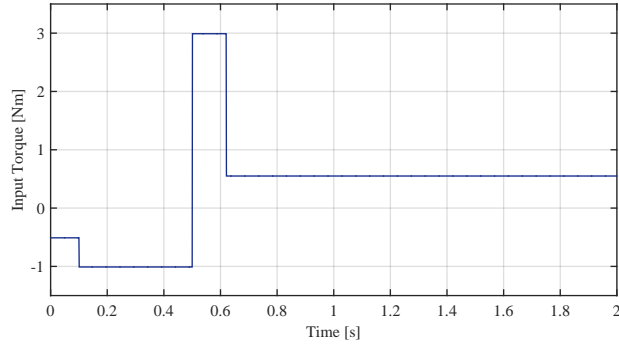Figure 2: L-shaped benchmark mechanism.



Figure 3: Input step torque signal.

The system has one rigid rotational degree of freedom and it has been modelled in Ansys$^{®}$ with 4, 8 and 16 *beam188* finite elements, i.e. 2, 4 and 8 elements for each of the two flexible rods that compose the L-system. It results a number of degrees of freedom for each subdivision equal to 30, 54 and 102 respectively. The mass $M$ and stiffness $K$ matrices of the complete model have been exported from Ansys$^{®}$ for each subdivision in beam elements and imported in Matlab$^{TM}$, where the reduction techniques have been applied. Then, the dynamic behaviour of the system has been numerically evaluated under two different input conditions: gravity and a torque signal, reported in Fig. 3.

For each subdivision of the mechanism in beam elements and for each modal reduction strategy, different simulations have been run, by varying the number of considered modes. In this way, not only the influence of elements number and of the reduction methodology but also the modal variables number can be evaluated.

The numerical simulations provided the dynamics of the system for a time of 2 seconds. An *ode45* variable-step solver, based on a Runge-Kutta integration scheme, has been adopted. Each simulation has been run three times in order to obtain an average value of computational time. For the simulations, a laptop running Windows 10 64 bit with an Intel$^{®}$ Core$^{TM}$ i7-4710HQ CPU @2.50 GHz and a 8 GB DDR3 installed RAM has been exploited.

## 5. Results and discussion

In this section, the results of the numerical simulations on the mechanism presented in Sect.4 are reported and discussed. Firstly, the different reduction techniques have been compared through the modal vector correlation parameters, then the dynamic behaviour is evaluated under both gravitational force and a step torque input.

### 5.1. Modal vector correlation parameters

In order to evaluate the accuracy of the reduced model in matching the mode frequencies and shapes of the full order model, three parameters have been here adopted: Modal Assurance Criterion (MAC) [1] [16] [18], Normal Cross-Orthogonality (NCO) [13] [15] [24] and Cross-Orthogonality (CO) [1]. The three parameters are defined as follows:

$$MAC_{i,j} = \frac{(\phi_i^T \phi_{r,j})^2}{(\phi_i^T \phi_i)(\phi_{r,j}^T \phi_{r,j})} \qquad NCO_{i,j} = \frac{(\phi_i^T M \phi_{r,j})^2}{(\phi_i^T M \phi_i)(\phi_{r,j}^T M \phi_{r,j})} \qquad CO_{i,j} = \phi_i^T M \phi_{r,j} \qquad (33)$$

where $\phi_i$ is the $i$-th eigenvector of the complete model, $\phi_{r,j}$ is the $j$-th eigenvector of the reduced model and $M$ is the mass matrix of the reduced model. By varying the indices $i$ and $j$, these parameters constitute a matrix, that will have values close to a identity matrix if the reduction is well-designed. In Fig.4 a graphical representation of the resultant matrices for the three parameters and the different reduction methods, in the case with 16 elements and 18 retained modes, is reported. In particular, in the techniques here implemented, the internal modes that have been chosen are those neither corresponding to the constrained end nor to the tip of the mechanism. It has to be noticed that in the Craig-Bampton, IMR and Guyan the choice of internal and secondary modes is fundamental for a good reduction, whereas the LSMR and MDM methods show a higher correspondence since they are based on a modal truncation approach.
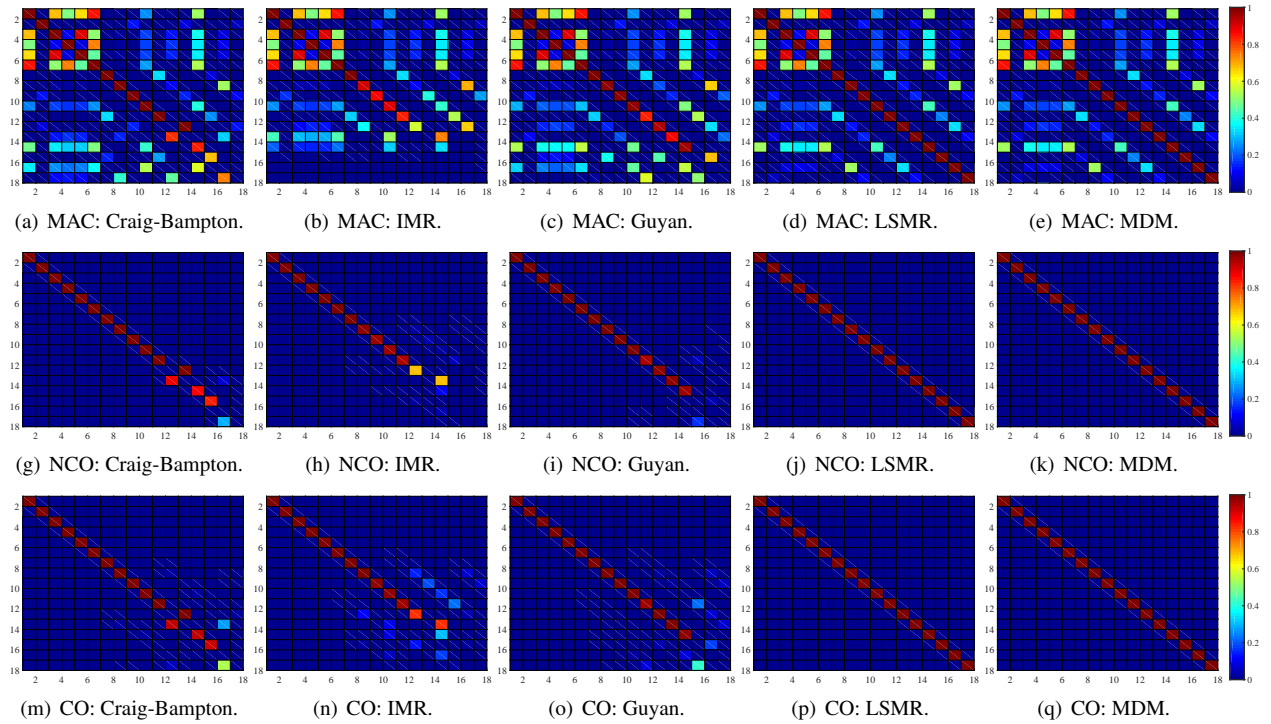


(a) MAC: Craig-Bampton.　(b) MAC: IMR.　(c) MAC: Guyan.　(d) MAC: LSMR.　(e) MAC: MDM.

(g) NCO: Craig-Bampton.　(h) NCO: IMR.　(i) NCO: Guyan.　(j) NCO: LSMR.　(k) NCO: MDM.

(m) CO: Craig-Bampton.　(n) CO: IMR.　(o) CO: Guyan.　(p) CO: LSMR.　(q) CO: MDM.

Figure 4: MAC, NCO and CO for the different methods, case with 16 elements and 18 considered modes.

### 5.2. Gravitational force input

In Fig.5 the tip Z-coordinate acceleration of the L-shaped mechanism under gravity in the frequency domain is reported. In particular, the case with 16 elements and 18 considered modes is shown. A good agreement between the different reduction techniques and the complete model in the first resonance peaks can be found, whereas, by considering the peak at almost 160 $Hz$, Craig-Bampton is the only method that accurately reproduces the dynamics of the full model. In Tables 1 and 2 the average computational times for the mechanism under gravity force are reported.
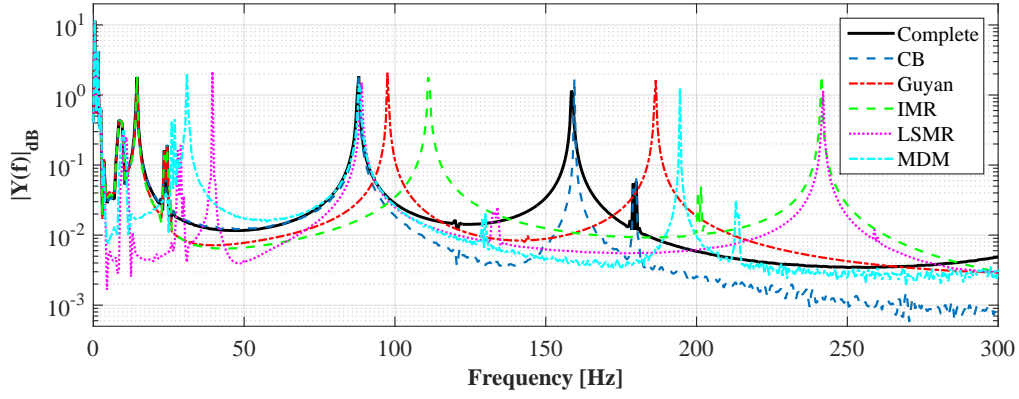
Figure 5: Comparison of the tip Z-coord. acceleration under gravity, case with 16 el. and 18 considered modes.

Table 1: Average computational time [s], mechanism under gravity, complete models.

| 4 el. (30 m.) | 8 el. (54 m.) | 16 el. (102 m.) |
|---|---|---|
| 1602,14 | 4046,99 | 16102,97 |

Table 2: Average computational time [s], mechanism under gravity.

| Method | Elements | Modes | | | | | |
|---|---|---|---|---|---|---|---|
| | | 8 | 10 | 12 | 14 | 16 | 18 |
| Craig-Bampton | 4 | 2,58 | 5,96 | 9,02 | 169,23 | 571,00 | 902,21 |
| | 8 | 3,12 | 5,13 | 13,49 | 32,38 | 51,20 | 89,75 |
| | 16 | 3,20 | 4,70 | 11,55 | 26,71 | 46,74 | 79,76 |
| IMR | 4 | 2,58 | 6,10 | 9,05 | 453,90 | 469,97 | 1079,11 |
| | 8 | 3,15 | 5,30 | 21,44 | 63,87 | 76,50 | 189,87 |
| | 16 | 1,85 | 5,82 | 13,60 | 176,38 | 322,75 | 502,47 |
| Guyan | 4 | 3,64 | 6,34 | 9,63 | 173,44 | 417,39 | 459,74 |
| | 8 | 2,55 | 5,74 | 18,87 | 28,04 | 94,64 | 297,22 |
| | 16 | 3,40 | 5,42 | 18,48 | 23,31 | 100,36 | 305,73 |
| LSMR | 4 | 2,59 | 6,04 | 9,18 | 181,77 | 255,96 | 421,53 |
| | 8 | 3,17 | 5,14 | 16,28 | 23,16 | 474,67 | 517,33 |
| | 16 | 3,22 | 4,80 | 15,02 | 19,77 | 629,20 | 1158,22 |
| MDM | 4 | 2,60 | 5,84 | 9,60 | 178,36 | 251,26 | 515,40 |
| | 8 | 3,08 | 5,02 | 16,26 | 23,50 | 28,45 | 74,06 |
| | 16 | 3,20 | 4,78 | 14,18 | 18,33 | 37,01 | 48,60 |

## 5.3. Step torque input

Fig.6 reports the Fast Fourier Transform of the tip Z-coordinate of the L-shaped system for the different reduction techniques in the case of step torque input. A good agreement between the complete model signal and the reduced ones can be appreciated in the first two resonance peaks, whereas Craig-Bampton seems to be the method that best matches the full model behaviour. Computational times are reported in Tables 3 and 4 for the complete and the reduced models respectively. As expected, a time reduction can be noticed by increasing the model elements at constant number of retained modes, since lower frequencies are, in general, taken into account. Furthermore, Craig-Bampton and MDM appear to be the methods that reduce at best the computational time.

Table 3: Average computational time [s], mechanism under torque input, complete models.

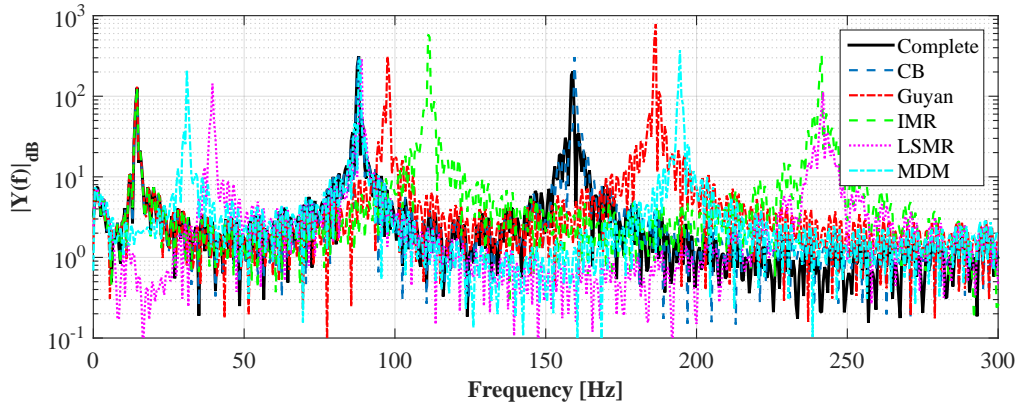| 4 el. (30 m.) | 8 el. (54 m.) | 16 el. (102 m.) |
|---|---|---|
| 1703,26 | 4110,21 | 17754,19 |

Figure 6: Comparison of the tip Z-coord. acceleration with torque input, case with 16 el. and 18 considered modes.

Table 4: Average computational time [s], mechanism under torque input.

| Method | Elements | Modes | | | | | |
|---|---|---|---|---|---|---|---|
| | | 8 | 10 | 12 | 14 | 16 | 18 |
| Craig-Bampton | 4 | 3,40 | 6,10 | 11,34 | 167,59 | 574,99 | 919,16 |
| | 8 | 3,30 | 4,39 | 13,00 | 33,73 | 50,71 | 89,66 |
| | 16 | 3,34 | 4,49 | 11,66 | 28,89 | 47,63 | 80,72 |
| IMR | 4 | 3,41 | 6,08 | 10,97 | 459,32 | 482,43 | 1092,52 |
| | 8 | 3,30 | 4,87 | 24,74 | 66,13 | 107,50 | 184,80 |
| | 16 | 2,69 | 5,83 | 15,14 | 171,01 | 316,48 | 510,80 |
| Guyan | 4 | 3,64 | 6,11 | 11,23 | 172,24 | 436,26 | 465,36 |
| | 8 | 3,41 | 5,16 | 20,70 | 30,67 | 98,44 | 292,73 |
| | 16 | 3,40 | 5,40 | 21,42 | 29,57 | 110,34 | 301,42 |
| LSMR | 4 | 3,33 | 6,10 | 11,33 | 184,68 | 229,75 | 408,88 |
| | 8 | 3,45 | 4,57 | 18,61 | 22,43 | 498,42 | 555,91 |
| | 16 | 3,44 | 4,43 | 16,56 | 20,03 | 637,77 | 1176,80 |
| MDM | 4 | 3,33 | 6,02 | 11,31 | 180,71 | 230,76 | 554,30 |
| | 8 | 3,39 | 4,60 | 18,89 | 24,11 | 31,09 | 80,87 |
| | 16 | 3,45 | 4,24 | 16,43 | 19,59 | 39,99 | 47,31 |

## 6. Conclusion and future works

In this paper, a first comparison of different model order reduction techniques using an ERLS formulation has been presented. In order to evaluate the accuracy of MOR methodologies, they have been applied on a L-shaped mechanism excited under gravity and by means of a torque input. The results have been compared in terms of vector correlation methods, dynamics behaviour in frequency domain and computational time showing advantages and disadvantages of the different considered MOR techniques. In further developments of this work, model order reduction techniques will be applied to a two (or more) DoFs multibody system with different subdivision in finite element domains. Furthermore, more techniques will be considered and a deeper analysis of the choice of internal modes will be performed.

## Acknowledgments

## References

[1] G.S. Aglietti, S. Redi, S.J.I. Walker, and A. Kiley. Robustness of the orthogonality checks on a satellite fem using a serep test analysis model. In *Proc. of the 24th Int. Conf. on Noise and Vibration Engineering*, 2010.

[2] M.S. Allen, R.L. Mayes, and E.J. Bergman. Experimental modal substructuring to couple and uncouple substructures with flexible fixtures and multi-point connections. *J. of Sound and Vibration*, 329(23):4891–4906, 2010.

[3] M.C.C. Bampton and R.R. Craig, JR. Coupling of substructures for dynamic analyses. *Aiaa Journal*, 6(7):1313–1319, 1968.

[4] B. Besselink, U. Tabak, A. Lutowska, N. Van De Wouw, H. Nijmeijer, D.J. Rixen, M.E. Hochstenbach, and W.H.A. Schilders. A comparison of model reduction techniques from structural dynamics, numerical mathematics and systems and control. *Journal of Sound and Vibration*, 332(19):4403–4422, 2013.

[5] P. Boscariol, P. Gallina, A. Gasparetto, M. Giovagnoni, L. Scalera, and R. Vidoni. Evolution of a dynamic model for flexible multibody systems. In *Advances in Italian Mechanism Science*, pages 533–541. Springer, 2017.

[6] P. Boscariol, A. Gasparetto, M. Giovagnoni, A.K. Moosavi, and R. Vidoni. On the modeling of flexible-link robots: First experimental validation of an erls-fem dynamic model. In *Mechatronics (ICM), 2013 IEEE International Conference on*, pages 298–302. IEEE, 2013.

[7] P. Boscariol, A. Gasparetto, L. Scalera, and R. Vidoni. Efficient closed-form solution of the kinematics of a tunnel digging machine. *Journal of Mechanisms and Robotics*, 9(3):031001, 2017.

[8] R. Caracciolo, D. Richiedei, and A. Trevisani. Experimental validation of a model-based robust controller for multi-body mechanisms with flexible links. *Multibody System Dynamics*, 20(2):129–145, September 2008.

[9] O. Flodén, K. Persson, and G. Sandberg. Reduction methods for the dynamic analysis of substructure models of lightweight building structures. *Computers & Structures*, 138:49–61, 2014.

[10] A. Gasparetto. Accurate modelling of a flexible-link planar mechanism by means of a linearized model in the state-space form for design of a vibration controller. *Journal of Sound and Vibration*, 240(2):241–262, 2001.

[11] R.J. Guyan. Reduction of stiffness and mass matrices. *AIAA journal*, 3(2):380–380, 1965.

[12] P. Koutsovasilis and M. Beitelschmidt. Comparison of model reduction techniques for large mechanical systems. *Multibody System Dynamics*, 20(2):111–128, 2008.

[13] N.A.J. Lieven and T.P. Waters. Error location using normalised orthogonality. In *Proceedings-Spie The International Society For Optical Engineering*, pages 761–761. Spie International Society For Optical, 1994.

[14] C. Nowakowski, J. Fehr, M. Fischer, and P. Eberhard. Model order reduction in elastic multibody systems using the floating frame of reference formulation. *IFAC Proceedings Volumes*, 45(2):40–48, 2012.

[15] I. Palomba, D. Richiedei, and A. Trevisani. Mode selection for reduced order modeling of mechanical systems excited at resonance. *International Journal of Mechanical Sciences*, 114:268–276, 2016.

[16] M. Pastor, M. Binda, and T. Harčarik. Modal assurance criterion. *Procedia Engineering*, 48:543–548, 2012.

[17] Z.Q. Qu. *Model order reduction techniques with applications in finite element analysis*. Springer Science & Business Media, 2013.

[18] D. Roettgen, B. Seeger, W.C. Tai, S. Baek, T. Dossogne, M. Allen, R. Kuether, M.R.W. Brake, and R. Mayes. A comparison of reduced order modeling techniques used in dynamic substructuring. In *Dynamics of Coupled Structures, Volume 4*, pages 511–528. Springer, 2016.

[19] C.V.S. Sastry, D.R. Mahapatra, S. Gopalakrishnan, and T.S. Ramamurthy. An iterative system equivalent reduction expansion process for extraction of high frequency response from reduced order finite element model. *Computer Methods in Applied Mechanics and Engineering*, 192(15):1821–1840, 2003.

[20] A.A. Shabana. Flexible multibody dynamics: Review of past and recent developments. *Multibody System Dynamics*, 1:189–222, 1997.

[21] R. Vidoni, P. Gallina, P. Boscariol, A. Gasparetto, and M. Giovagnoni. Modeling the vibration of spatial flexible mechanisms through an equivalent rigid-link system/component mode synthesis approach. *Journal of Vibration and Control*, published online, 2015.

[22] R. Vidoni, A. Gasparetto, and M. Giovagnoni. Design and implementation of an erls-based 3-d dynamic formulation for flexible-link robots. *Robot. Comput.-Integr. Manuf.*, 29(2):273–282, 2013.

[23] R. Vidoni, A. Gasparetto, and M. Giovagnoni. A method for modeling three-dimensional flexible mechanisms based on an equivalent rigid-link system. *Journal of Vibration and Control*, 20(4):483–500, 2014.

[24] V. Zeman and M. Hajžman. Usage of the generalized modal synthesis method in dynamics of machines. *Engineering Mechanics*, 14(1-2):45–54, 2007.